

# Subamolide E from *Cinnamomum subavenium* Induces Sub-G1 Cell-Cycle Arrest and Caspase-Dependent Apoptosis and Reduces the Migration Ability of Human Melanoma Cells

Hui-Min Wang,<sup>†</sup> Chien-Chih Chiu,<sup>‡</sup> Pei-Fang Wu,<sup>†</sup> and Chung-Yi Chen<sup>\*,§</sup>

<sup>†</sup>Department of Fragrance and Cosmetic Science, and <sup>‡</sup>Department of Biotechnology, Kaohsiung Medical University, 100, Shih-Chuan 1st Road, San-Ming District, Kaohsiung 807, Taiwan, Republic of China

<sup>§</sup>Department of Medical Laboratory Science and Biotechnology, School of Medical and Health Sciences, Fooyin University, 151, Ching-Hsueh Road, Ta-Liao District, Kaohsiung 831, Taiwan, Republic of China

**ABSTRACT:** The aim of this work was to investigate the anticancer cytotoxic effects of natural compound subamolide E on the human skin cancer melanoma A375.S2 cells. Subamolide E was isolated from *Cinnamomum subavenium* and demonstrated cytotoxicities in the cell-growth assay at concentration ranges from 0 to 100  $\mu$ M at 24 h. Propidium iodide staining and flow cytometry analyses were used to evaluate cell-cycle distribution and found that subamolide E caused DNA damage in the sub-G1 phase with a dose-dependent manner after 24 h of treatment. According to the western blot result, subamolide-E-treated cells with the increase of caspase-dependent apoptotic proteins induced related pathway mechanisms. Subamolide E also showed antimigratory activities of A375.S2 cells on the wound-healing assay. Finally, subamolide E demonstrated minor cytotoxicities to normal human skin cells (keratinocytes, melanocytes, and fibroblasts); therefore, it is a potential chemotherapeutic agent against skin melanoma.

**KEYWORDS:** Subamolide E, melanoma, antiproliferation, cell-cycle arrest, caspase-dependent apoptosis, cell migration

## INTRODUCTION

Human skin is normally contacted with damage stress, which is produced by external and intrinsic sources, such as ultraviolet (UV) radiation, free radicals, and reactive oxygen species.<sup>1–6</sup> There are many studies about the skin exposed to oxidative stress or UV radiation and are responsible for aging or tumorigenesis.<sup>7,8</sup> Melanoma, a malignant tumor of epidermal melanocytes, is one of the most deadly skin cancers.<sup>9,10</sup> Within the past several decades, the occurrences of cutaneous malignant melanoma have increased because it has a strong propensity to metastasize and, therefore, is one of the most aggressive skin cancers.<sup>11,12</sup> Unlike other cancers, malignant melanoma is not easy to treat with surgery, radiotherapy, or chemotherapy.<sup>13</sup> A good chemotherapeutic agent will be a naturally occurring agent and can induce cytotoxicity in cancer cells.

*Cinnamomum subavenium* Miq. (Lauraceae) is a medium-sized evergreen tree plant and usually visible in the central to southern mainland of China, Burma, Cambodia, Indonesia, Malaysia, and Taiwan.<sup>14</sup> Upon the continuation of a study toward the research programs of a biochemical-active component from Formosan lauraceous plants, one butanolide, namely, subamolide E [(4*R*,3*E*)-4-hydroxy-5-methylene-3-undecylidenedihydrofuran-2-one], was isolated (Figure 1).<sup>15</sup> Subamolide E has been proven to exert an inhibitory effect on proliferation in colon carcinoma SW480.<sup>16</sup> In the study, we proposed a hypothesis that subamolide E is a potential component for developing an anticancer drug against A375.S2 cells. The effects of subamolide E on cell growth, cell-cycle progression, apoptotic mechanism, and migration effects were examined. Our data proved that subamolide E could be beneficial in the chemotherapy of human melanoma and without significant cytotoxicity to normal skin cells.

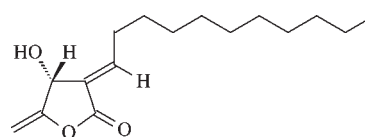


Figure 1. Compound structures of subamolide E from *C. subavenium*.

## MATERIALS AND METHODS

**Plant Material.** The leaves of *C. subavenium* were collected from Wulai Hsiang, Taipei County, Taiwan, in May, 2005. These voucher specimens (Cinnamo. 5) were characterized by Dr. Yen-Ray Hsui of the Chungpu Research Center, Taiwan Forestry Research Institute, Chiayi, Taiwan, and deposited in the Department of Medical Laboratory Science and Biotechnology, School of Medical and Health Sciences, Fooyin University, Kaohsiung County, Taiwan, Republic of China.

**Extraction and Isolation.** The air-dried leaves of *C. subavenium* (11.0 kg) were extracted by methanol (50 L  $\times$  6) at room temperature, and a methanol extract (326.5 g) was obtained upon concentration under reduced pressure. The methanol extract, suspended in H<sub>2</sub>O (1 L), was partitioned with chloroform (2 L  $\times$  5) to give fractions soluble in chloroform (198.5 g) and H<sub>2</sub>O (101.2 g). The chloroform-soluble fraction (198.5 g) was chromatographed over silica gel (800 g, 70–230 mesh) using *n*-hexane/ethyl acetate/methanol mixtures as eluents to produce five fractions. Fraction 1 (9.33 g) was subjected to silica gel chromatography by eluting with *n*-hexane/ethyl acetate (20:1) and enriched with ethyl acetate to furnish five fractions (1–1–1–5).

Received: May 15, 2011

Revised: June 21, 2011

Accepted: June 27, 2011

Published: June 27, 2011

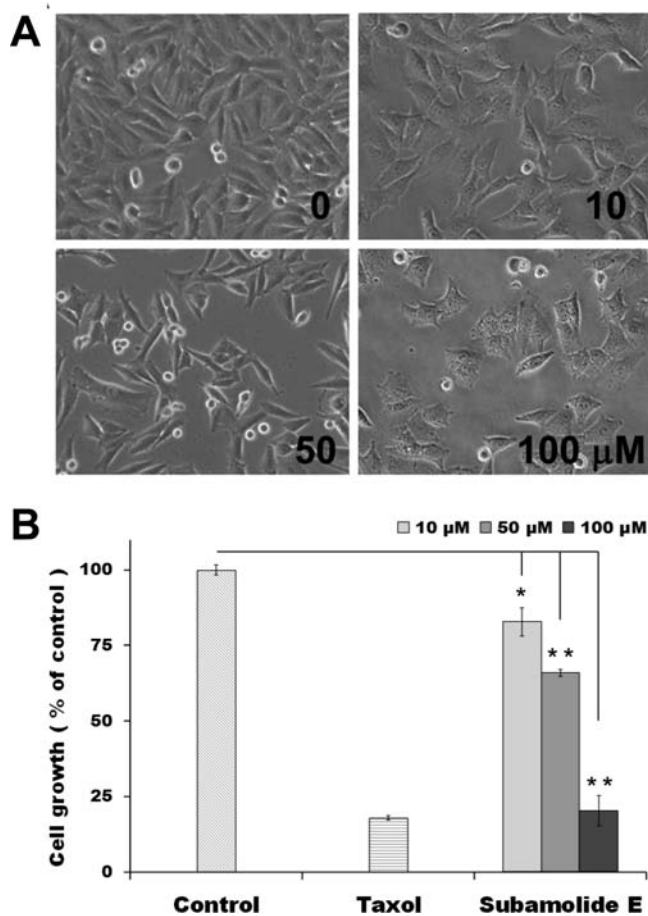


**Figure 2.** Effects of subamolide E on A375.S2 cell growth measured by the MTT assay. (A) Photos of A375.S2 cells were taken with a bright field microscope, and the magnification was 200 $\times$ . (B) Quantification of the cell-growth inhibition of subamolide E on A375.S2 cells, and cells were treated for 24 h with 10, 50, and 100  $\mu$ M. Control with no testing sample (slash lines), and Taxol with 0.5  $\mu$ M (horizontal lines). The data represented the mean  $\pm$  SD of triplicate values for three independent experiments. Bars = SD, with (\*)  $p < 0.05$  and (\*\*)  $p < 0.01$  against subamolide E treatment.

Fraction 1–2 (3.02 g) was subjected to silica gel chromatography, eluted with *n*-hexane/ethyl acetate (50:1), and enriched gradually with ethyl acetate, to obtain three fractions (1–2–1–1–2–3). Fraction 1–2–2 (2.26 g), eluted with *n*-hexane/ethyl acetate (40:1), was further separated using silica gel column chromatography and preparative thin-layer chromatography [TLC, *n*-hexane/ethyl acetate (30:1)] and gained subamolide E (51 mg).<sup>15</sup>

**General Experimental Procedures.** Melting points were determined using a Yanagimoto micromelting point apparatus and are uncorrected. Optical rotations were measured with a JASCO DIP-370 digital polarimeter. UV spectra were obtained in methyl cyanide using a JASCO V-530 spectrophotometer. The infrared (IR) spectra were measured on a Hitachi 260-30 spectrophotometer. <sup>1</sup>H (400 MHz, using deuterated chloroform as the solvent for measurement), <sup>13</sup>C (100 MHz), distortionless enhancement by polarization transfer (DEPT), heteronuclear correlation (HETCOR), correlation spectroscopy (COSY), nuclear Overhauser effect spectrometry (NOESY), and heteronuclear multiple-bond correlation (HMBC) nuclear magnetic resonance (NMR) spectra were obtained on a Unity Plus Varian NMR spectrometer. Low-resolution fast atom bombardment mass spectrometry (LRFABMS) and low-resolution electron impact mass spectrometry (LREIMS) were

obtained with a JEOL JMS-SX/SX 102A mass spectrometer or a Quattro gas chromatography–mass spectrometry (GC–MS) spectrometer with a direct inlet system. High-resolution fast atom bombardment mass spectrometry (HRFABMS) and high-resolution electron impact mass spectrometry (HREIMS) were measured on a JEOL JMS-HX 110 mass spectrometer. Silica gel 60 (Merck, 230–400 mesh) was used for column chromatography. Precoated silica gel plates (Merck, Kieselgel 60 F-254, 0.20 mm) were used for analytical TLC, and precoated silica gel plates (Merck, Kieselgel 60 F-254, 0.50 mm) were used for preparative TLC. Spots were detected by spraying with 50% H<sub>2</sub>SO<sub>4</sub> and then heating on a hot plate. The structure of subamolide E was identified by spectroscopic analysis (purity > 95%). This compound was identified by spectroscopic data analysis.<sup>15</sup>

**Chemicals and Reagents.** Dimethyl sulfoxide (DMSO), 3-(4,5-dimethylthiazol-2-yl)-2,5-diphenyltetrazolium bromide (MTT), and propidium iodide (PI) were purchased from Sigma-Aldrich Company (St. Louis, MO). RPMI-1640, antibiotics, and other supplements for cell cultures were purchased from Invitrogen (Carlsbad, CA). Fetal bovine serum (FBS) and Dulbecco's modified Eagle's medium (DMEM) were obtained from Gibco BRL (Gaithersburg, MD). The human skin cancer cell line, A375.S2, was purchased from Bioresource Collection and Research Center (BCRC, Hsinchu, Taiwan, Republic of China). The antibody against caspase-8 was purchased from Anaspec (San Jose, CA), and antibodies against cleaved caspase-3, caspase-7, caspase-9, poly-(ADP-ribose) polymerase (PARP), and  $\beta$ -actin were purchased from Cell Signaling (Beverly, MA). Anti-mouse and anti-rabbit IgG peroxidase-conjugated secondary antibodies were purchased from Pierce (Rockford, IL). All other reagents and chemicals used were obtained in the purest forms possible from commercial sources.

**Cell Cultures.** A375.S2 cells were maintained in a monolayer culture at 37  $^{\circ}$ C and 5% CO<sub>2</sub> in DMEM supplemented with 10% FBS, 100 units/mL of penicillin, 100 mg/mL of streptomycin, and 0.25  $\mu$ g/mL of amphotericin B.<sup>6</sup> Stock solutions of subamolide E (1.0 M) were dissolved in DMSO, and various concentrations were prepared with a final DMSO concentration less than 0.5%.

Human keratinocytes were grown from foreskin primary culture, which was derived from Chung-Ho Memorial Hospital, Kaohsiung Medical University, Taiwan.<sup>2,3</sup> Human keratinocytes were cultured in keratinocyte-SFM (Gibco, Gaithersburg, MD), supplemented with bovine pituitary extract (BPE) and human recombinant epidermal growth factor (EGF). The medium and growth supplement for keratinocytes contain  $\gamma$ -epidermal growth factor, BPE, insulin, fibroblast growth factor, and calcium (0.09 mM).

Neonatal foreskin primary human epidermal melanocytes (HEMn-MP) were purchased from Cascade Biologics, cultured in Medium 254 (Cascade Biologics, Portland, OR) and supplemented with human melanocyte growth supplement (HMGs).<sup>2,3</sup> The Medium 254 is a basal medium containing essential and non-essential amino acids, vitamins, organic compounds, trace minerals, and inorganic salts. The human melanocyte growth supplement contains BPE, FBS, bovine insulin, bovine transferrin, basic fibroblast growth factor, hydrocortisone, heparin, and phorbol 12-myristate 13-acetate.

The primary cultures of human skin fibroblasts were cultured in the DMEM medium.<sup>2,3</sup> All cells were incubated at 37  $^{\circ}$ C under a humidified atmosphere of 5% CO<sub>2</sub> in air and routine passage by trypsinization.

**Cell Proliferation Assay.** The effects of compounds on cell growths were according to the MTT assay procedures.<sup>4</sup> The method is based on the ability of a mitochondrial dehydrogenase enzyme from viable cells to cleave the tetrazolium rings of the pale yellow MTT and form impermeable crystals of a dark-blue formazan, thus resulting in accumulation within healthy cells. Briefly, cells were seeded in 96-well microplates at a density of  $7 \times 10^3$  cells/well. The medium was then changed, and cells were maintained in either solvent alone (control cells) or in the presence of the indicated drug concentrations in a final volume

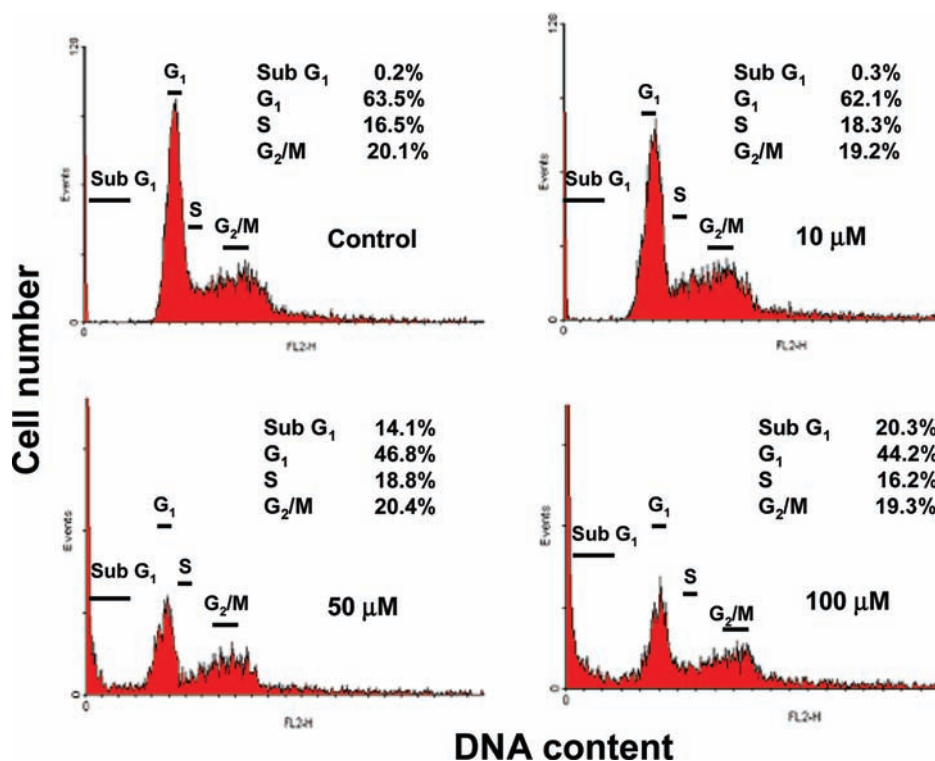


**Figure 3.** Effects of subamolide E on the cell cycle of the A375.S2 cell line. A375.S2 cells were treated with the indicated concentrations of subamolide E for 24 h. After treatment, cells were collected, fixed with methanol, stained with PI, and analyzed by flow cytometry. Data on each sample represent the percentages of sub-G<sub>1</sub>, G<sub>1</sub>, S, and G<sub>2</sub>/M. Analyses were performed at least 3 times, and a representative experiment is presented.

of 100  $\mu$ L in 10% FBS culture medium. The testing samples were dissolved in sterile DMSO to treat a working concentration. Each concentration was added to a microplate in three replicates and incubated under the same conditions as above for 24 h. After 24 h of incubation, the medium was replaced with 100  $\mu$ L of fresh medium including 0.5 mg/mL MTT. The microplate was cultured in a 37 °C incubator filled with 5% CO<sub>2</sub> for 2 h. Each precipitate in a specific dish was dissolved in 100  $\mu$ L of DMSO to dissolve the purple formazan crystals. After the dishes were gently shaken for 10 min in the dark to ensure maximal dissolution of formazan crystals, the absorbance (*A*) values of the supernatant were measured at 595 nm (UV-vis, BioTek, Winooski, VT). Cell growth was calculated as

$$\frac{(A_{\text{sample}} - A_{\text{blank}})}{(A_{\text{control}} - A_{\text{blank}})} \times 100\%$$

**DNA Damage and Cell-Cycle Analysis on the A375.S2 Cell Line.** To determine the phase distribution of DNA content, PI staining was performed as described.<sup>16,17</sup> A375.S2 cells were cultured in 100 mm tissue-culture dishes. The monolayer was treated with various concentrations of subamolide E for 24 h. Adherent and floating cells were collected after treatment, washed twice with phosphate-buffered saline (PBS), then fixed with PBS/methanol (1:2, v/v) solution, and stored at 4 °C for at least 18 h. After centrifugation at 700 rpm for 5 min at 4 °C, the cell pellet was stained with 10  $\mu$ g/mL PI and 10  $\mu$ g/mL RNase A in PBS buffer for 15 min at room temperature in the dark environment. DNA fluorescence of PI-stained cells was evaluated by excitation at 488 nm and detected through a 630/22 nm band-pass filter. Analyses were performed with FACScan flow cytometry (Becton-Dickinson, Mansfield, MA) and Cell-Quest and Modfit software to evaluate the extent of DNA damage and the percentage of cells in various phases (sub-G<sub>1</sub>, G<sub>1</sub>, S, G<sub>2</sub>, and M) of the cell cycle.<sup>16,17</sup>

**Western Blot Analysis.** A total of  $1 \times 10^6$  cells were treated with compound 1-3 or the vehicle control for 24 h, respectively. The cells were harvested and lysed with lysis buffer<sup>18</sup> [50 mM Tris-HCl at pH 7.5, 137 mM sodium chloride, 1 mM ethylenediaminetetraacetic acid (EDTA), 1% Nonidet P-40, 10% glycerol, 0.1 mM sodium orthovanadate, 10 mM sodium pyrophosphate, 20 mM  $\beta$ -glycerophosphate, 50 mM sodium fluoride, 1 mM phenylmethylsulfonyl fluoride, 2  $\mu$ M leupeptin, and 2  $\mu$ g/mL aprotinin]. Lysates were centrifuged at 20000g for 30 min, and the protein concentration in the supernatant was determined with the bicinchoninic acid (BCA) protein assay kit (Pierce, Rockford, IL). Equal amounts of protein were separated by sodium dodecyl sulfate–polyacrylamide gel electrophoresis (SDS–PAGE) and then electrotransferred to a nitrocellulose membrane (PALL Life Science, Ann Arbor, MI). The membrane was blocked for 1 h with 5% nonfat milk in PBS-T buffer (PBS containing 0.1% Tween 20). The membranes were incubated with corresponding primary antibodies, washed twice with PBS, and then incubated with secondary antibodies against the corresponding primary antibodies. The signals were visualized using the chemiluminescence detection kit (Amersham, Piscataway, NJ).

**Cell Migration Assay.** The potential of cellular migration was determined by wound-healing migration assays, which was performed according to the methods reported<sup>19</sup>. In brief,  $5 \times 10^5$  cells were seed in 12-well plates and grown to complete confluence. A yellow 200  $\mu$ L plastic pipet tip was used to create a clean 1 mm wide wound area on a confluent monolayer culture, and then cells were treated with testing samples or PBS buffer. After 24 h, the wound gaps were photographed using inverted phase-contrast microscopy (TE2000-U, Nikon, Tokyo, Japan) equipped with NIS-Elements (Nikon) software. The migration and cell movement throughout the wound area were examined and calculated by the free software “TScratch” ([www.cse-lab.ethz.ch/software.html](http://www.cse-lab.ethz.ch/software.html)).<sup>20</sup>



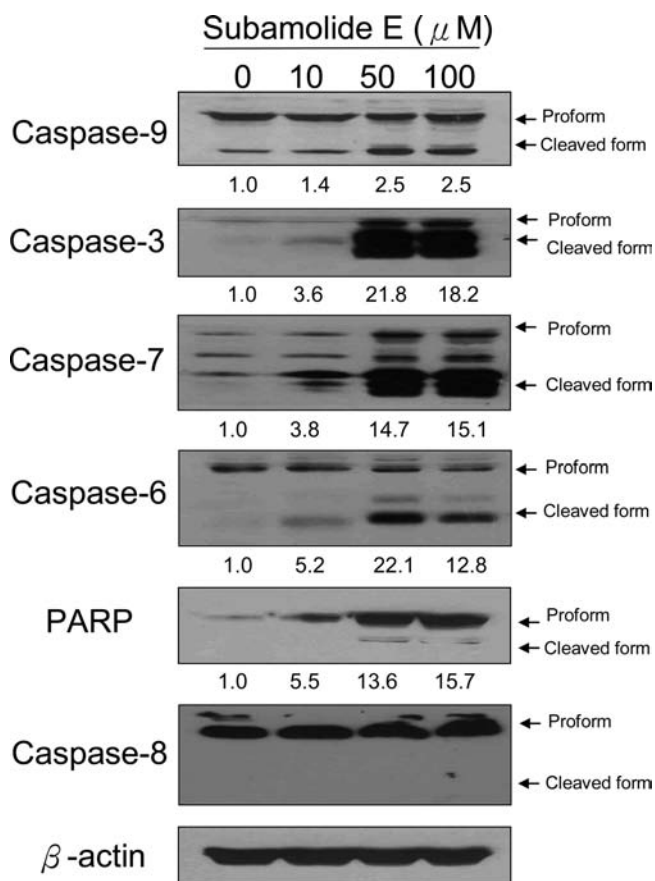


**Figure 4.** Western blotting of A375.S2 cells treated with subamolide E. Cells were cultured with subamolide E for 24 h. The apoptotic-related proteins caspase-3, caspase-6, caspase-7, caspase-8, and caspase-9 and the cleaved form of PARP were determined by western blot analysis, as described in the Materials and Methods.  $\beta$ -actin was an internal control.

**Statistical Analysis.** All data were presented as the mean  $\pm$  standard deviation (SD), and the Student's *t* test was used to identify the mean difference between the two groups.

## RESULTS AND DISCUSSION

### Antiproliferative Effects of Subamolide E on A375.S2 Cell.

The main reason of the death on a patient is due to the tumor proliferation and metastasis. Therefore, it is urgent to find valuable and significant novel biomedical components for anticancer therapies. To evaluate the effects of subamolide E on cancer cytotoxicity, the melanoma cells were treated at 0 (control, with PBS buffer), 10, 50, and 100  $\mu$ M concentrations (Figure 2). Morphological changes were observed by a bright field microscope, and the magnification was 200 $\times$  without staining (Figure 2A). The MTT assay illustrated the anti-cell proliferation of subamolide E on A375.S2 cells for 24 h treatments (Figure 2B). The anticancer drug, Taxol, has shown to cause cells at  $G_2/M$  in a variety of human cancer cell lines, including breast cancer,<sup>21</sup> lung cancer,<sup>22</sup> and melanoma.<sup>15,23</sup> Therefore, Taxol was used as a positive control in our study. The proliferation of the human melanoma cell was inhibited by subamolide E in a dose-dependent manner from 0 to 100  $\mu$ M. We demonstrated the potent cytotoxic abilities on human skin melanoma cells of subamolide E.

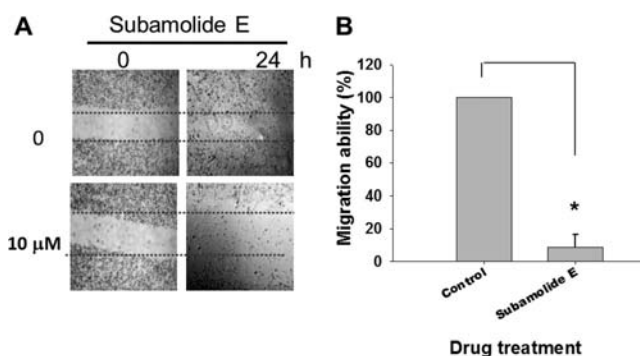


**Figure 5.** Migration inhibition of subamolide E treated on A375.S2 cells. The wound-healing assay was used to examine the effects of subamolide E on migration potential. (A)  $5 \times 10^5$  A375.S2 cells treated with subamolide E or PBS (as control), seeded in 12-well plates, and grown to complete confluence. Cells were then scraped with a 200  $\mu$ L plastic tip to produce a clean  $\sim 1$  mm wide wound area. Afterward, cells were permitted to migrate into the area of clearing for 24 h and photographed. (B) Quantification of the migration potential of subamolide-E- or PBS-treated cells. The migration and cell movement throughout the wound area were examined and calculated by the free software "TScratch" ([www.cse-lab.ethz.ch/software.html](http://www.cse-lab.ethz.ch/software.html)). Magnification = 100 $\times$ . Bars = SD, with (\*)  $p < 0.05$  against subamolide E treatment.

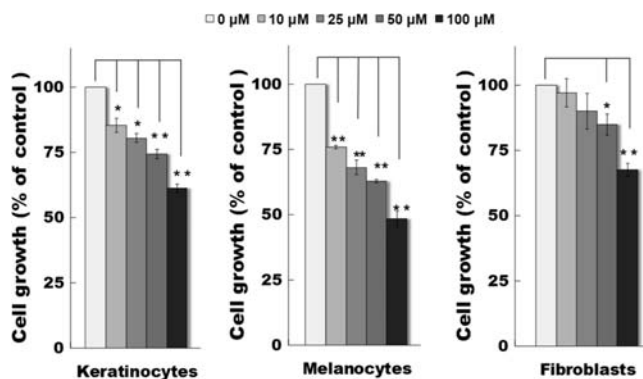


**Figure 6.** Normal human skin cell growth of epidermal keratinocytes, dermal melanocytes, and fibroblasts after treatments with various concentrations of subamolide E. Human keratinocytes were on the left side. Melanocytes were in the middle. Fibroblasts were on the right side. Bars = SD, with (\*)  $p < 0.001$  and (\*\*)  $p < 0.0005$  against subamolide E treatment.

### Assessment of Cell-Cycle Arrest and Sub- $G_1$ Accumulation.

We examined the influences on DNA of 0–100  $\mu$ M subamolide E, after 24 h of treatment, on the cancer A375.S2 cell, by PI staining followed by flow cytometry. The accumulation of the sub- $G_1$  population is considered as a biomarker for DNA damage, and the appearance of this peak is related to the presence of apoptosis. As shown in Figure 3, the sub- $G_1$  accumulation of the untreated control group was 0.22% and the DNA damage had a slight increase to 0.32% because of subamolide E at a concentration of 10  $\mu$ M. At the concentrations of 50 and 100  $\mu$ M, subamolide E induced DNA damages significantly and the sub- $G_1$  accumulation was increased to 14.1 and 20.3%, respectively. It had an obvious difference of about 100-fold at 100  $\mu$ M compared to the control group on the sub- $G_1$  phase.

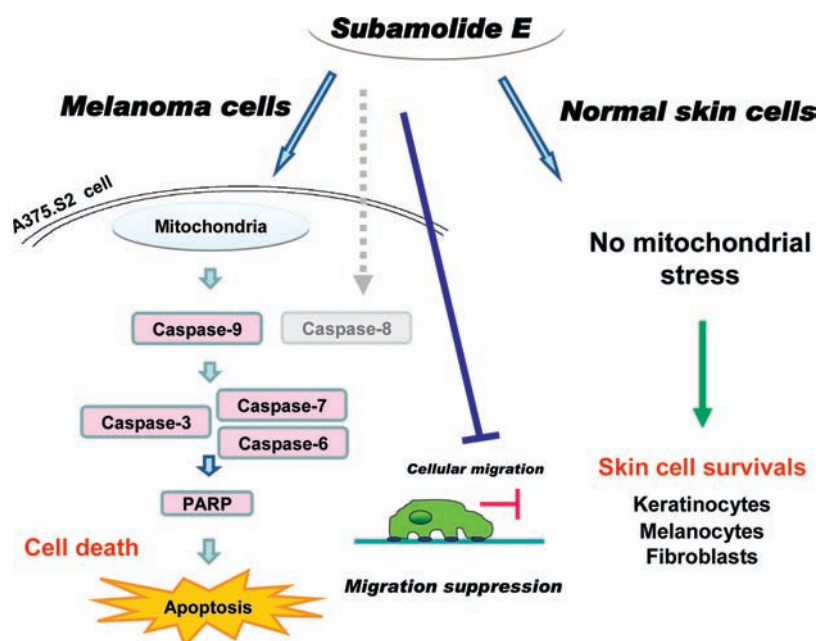


**Figure 7.** Proposed schematic diagram of subamolide E biofunctions on human skin cells, including the melanoma apoptotic pathway, migration inhibition, and normal cell survival.

**Effects of Mitochondrial-Mediated Caspase Cascade in Subamolide-E-Treated A375.S2 Cells.** The activations of caspases are essential for executing cell death by a variety of apoptotic stimuli.<sup>24,25</sup> Therefore, to evaluate the role played by caspase proteins in the apoptotic effect induced by subamolide E in human melanoma cells, the activations of caspase-9, caspase-3, caspase-7, caspase-6, and caspase-8 were examined after 24 h of treatment. Figure 4 showed that subamolide E increased the proteolytically activated forms of caspase-9, caspase-3, and caspase-7 dramatically following 50 and 100  $\mu\text{M}$ . However, no cleaved form of caspase-8 was observed even at the highest dose of subamolide E, suggesting that the death-receptor-mediated apoptotic pathway<sup>23</sup> was not involved or played a minor effect. In particular, the activities of caspase-3 and caspase-7 were enhanced significantly after subamolide E treatments.

**Protein Expression of the Cleavage of PARP in Subamolide-E-Treated A375.S2 Cells.** Another apoptotic-related protein was also evaluated on subamolide-E-treated human melanoma cells, as shown in Figure 4. The cleavage of PARP increased slightly at a higher dose of 50 and 100  $\mu\text{M}$  subamolide E. We inferred that subamolide E can cause the proteolytic activations of several caspase proteins and the proteolytic inactivation of PARP to hamper physiological behaviors of A375.S2 cells, and therefore, it can be useful as a potential herbal supplement for chemotherapeutics on human skin cancer.

**Cell Migration of A375.S2 Cells Inhibited by Subamolide E.** In normal human physiological conditions, cell migration plays a critical role for maintaining the development and homeostasis.<sup>26</sup> However, the deregulated migration of cancer cells is frequently responsible for the metastasis of malignant tumors.<sup>27</sup> The inhibition of A375.S2 cell migration through subamolide E was examined by a wound-healing assay and shown in Figure 5. Photographs in Figure 5A presented the migration of A375.S2 cells ( $5 \times 10^5$  cells) with various concentrations of subamolide E, and the quantification analysis was shown in Figure 5B. With the

treatment of subamolide E, cells were not permitted to migrate into the area of clearing for 24 h at concentrations of 10  $\mu\text{M}$ . A higher dosage than 10  $\mu\text{M}$  subamolide E led to an inhibitory effect on the cell survival of A375.S2 cells (migration data not shown). The quantitative assay demonstrated that the migratory potential of subamolide-E-treated cells at 24 h was 0.59-fold compared to the vehicle control, suggesting the efficient inhibitory effect of subamolide E. It might be concluded that the cell death damaging effect of subamolide E against skin cancer cells leads to growth inhibition as well as a depression in migration aptitude.

**Cytotoxicities of Subamolide E of Normal Human Skin Cells.** On the basis of the above findings, we targeted subamolide E from *C. subavenium* from a large number of plant component screenings of the anticancer assays. As a potent anticancer agent, the component should be harmless, without undesirable cytotoxic side effects. Considering the medical and therapeutic usage of subamolide E, the effects on normal cell growth are extensively important. Thus, we did an assessment on the cytotoxic properties of subamolide E on normal human skin cells, including epidermal keratinocytes, melanocytes, and dermal fibroblasts. Subamolide E was treated with various concentrations from 0 to 100  $\mu\text{M}$  to verify the dose-dependent effects. In Figure 6, three kinds of normal skin cells were exposed to a high dose (100  $\mu\text{M}$ ) of subamolide E and exhibited viabilities of more than 50% after 24 h of treatment. This result revealed that this compound had little discernible toxic properties to human epidermal and dermal cells.

Subamolide E presented inhibitory activities on the proliferation and migration of the human melanoma cell line to be a chemotherapeutic agent or potential natural lead compound. Additionally, subamolide E was not too harmful on the cell growth of keratinocytes, melanocytes, and fibroblasts. Taken together, we proposed biofunctions of subamolide E to A375.S2 and normal skin cells and demonstrated this in Figure 7.

## AUTHOR INFORMATION

### Corresponding Author

\*Telephone: +886-7-7811151-495. Fax: +886-7-7834548. E-mail: xx377@mail.fy.edu.tw.

### Funding Sources

This work was financially supported by the National Science Council of the Republic of China under Grants NSC-99-2221-E-037-006-MY3, NSC-98-2314-B-037-035, and NSC-97-2320-B-242-002-MY3 as well as the Kaohsiung Medical University under Grant KMU-Q098034, the Taiwan Tech Trek Program (2010), and the Academic Community about Industry Program.

## ACKNOWLEDGMENT

The authors thank Ching-Yi Tseng and Yu-Chen Chang for their assistance.

## REFERENCES

- Baldea, I.; Mocan, T.; Cosgarea, R. The role of ultraviolet radiation and tyrosine stimulated melanogenesis in the induction of oxidative stress alterations in fair skin melanocytes. *Exp. Oncol.* **2009**, *31*, 200–208.
- Wang, H. M.; Chen, C. Y.; Wen, Z. H. Identifying melanogenesis inhibitors from *Cinnamomum subavenium* with *in vitro* and *in vivo* screening systems by targeting the human tyrosinase. *Exp. Dermatol.* **2011**, *20*, 242–248.
- Wang, H. M.; Chen, C. Y.; Chen, C. Y.; Ho, M. L.; Chou, Y. T.; Chang, H. C.; Lee, C. H.; Wang, C. Z.; Chu, I. M. (–)-N-Formylanoinine from *Michelia alba* as human tyrosinase inhibitor and antioxidant. *Bioorg. Med. Chem.* **2010**, *18*, 5241–5247.
- Wang, H. M.; Pan, J. L.; Chen, C. Y.; Chiu, C. C.; Yang, M. H.; Chang, H. W.; Chang, J. S. Identification of anti-lung cancer extract from *Chlorella vulgaris* C–C by antioxidant property using supercritical carbon dioxide extraction. *Process Biochem.* **2010**, *45*, 1865–1872.
- Wang, S. Q.; Setlow, R.; Berwick, M.; Polsky, D.; Marghoob, A. A.; Kopf, A. W.; Bart, R. S. Ultraviolet A and melanoma: A review. *J. Am. Acad. Dermatol.* **2001**, *44*, 837–846.
- Chen, C. Y.; Kuo, P. L.; Chen, Y. H.; Huang, J. C.; Ho, M. L.; Lin, R. J.; Chang, J. S.; Wang, H. M. Tyrosinase inhibition, free radical scavenging, antimicroorganism and anticancer proliferation activities of *Sapindus mukorossi* extracts. *J. Taiwan Inst. Chem. Eng.* **2010**, *41*, 129–135.
- Briganti, S.; Picardo, M. Antioxidant activity, lipid peroxidation and skin diseases. What's new. *J. Eur. Acad. Dermatol. Venereol.* **2003**, *17*, 663–669.
- Picardo, M.; Grammatico, P.; Roccella, F.; Roccella, M.; Grandinetti, M.; Del Porto, G.; Passi, S. Imbalance in the antioxidant pool in melanoma cells and normal melanocytes from patients with melanoma. *J. Invest. Dermatol.* **1996**, *107*, 322–326.
- Weinstock, M. A. Early detection of melanoma. *J. Am. Med. Assoc.* **2000**, *284*, 886–889.
- Halachmi, S.; Gilchrist, B. A. Update on genetic events in the pathogenesis of melanoma. *Curr. Opin. Oncol.* **2001**, *13*, 129–136.
- Jemal, A.; Devesa, S. S.; Hartge, P.; Tucker, M. A. Recent trends in cutaneous melanoma incidence among whites in the United States. *J. Natl. Cancer Inst.* **2001**, *93*, 678–683.
- Tran, H.; Chen, K.; Shumack, S. Epidemiology and aetiology of basal cell carcinoma. *Br. J. Dermatol.* **2003**, *149* (Supplement 66), 50–52.
- White, N.; Knight, G. E.; Butler, P. E.; Burnstock, G. An *in vivo* model of melanoma: Treatment with ATP. *Purinergic Signalling* **2009**, *5*, 327–333.
- Liao, J. C. *Lauraceae in Flora of Taiwan*, 2nd ed.; Editorial Committee of the Flora of Taiwan: Taipei, Taiwan, 1996; Vol. 2, pp 443–483.
- Wang, H. M.; Chou, Y. T.; Hong, Z. L.; Chen, H. A.; Chang, Y. C.; Yang, W. L.; Chang, H. C.; Mai, C. T.; Chen, C. Y. Bioconstituents

from stems of *Synsepalum dulcificum* Daniell (Sapotaceae) inhibit human melanoma proliferation, reduce mushroom tyrosinase activity and have antioxidant properties. *J. Taiwan Inst. Chem. Eng.* **2011**, *42*, 204–211.

(16) Kuo, S. Y.; Hsieh, T. J.; Wang, Y. D.; Lo, W. L.; Hsui, Y. R.; Chen, C. Y. Cytotoxic constituents from the leaves of *Cinnamomum subavenium*. *Chem. Pharm. Bull.* **2008**, *56*, 97–101.

(17) Chiu, C. C.; Li, C. H.; Fuh, T. S.; Chen, W. L.; Huang, C. S.; Chen, L. J.; Ung, W. H.; Fang, K. The suppressed proliferation and premature senescence by ganciclovir in p53-mutated human non-small-lung cancer cells acquiring herpes simplex virus-thymidine kinase cDNA. *Cancer Detect. Prev.* **2005**, *29*, 286–293.

(18) Chen, B. H.; Chang, H. W.; Huang, H. M.; Chong, I. W.; Chen, J. S.; Chen, C. Y.; Wang, H. M. (–)-Anonaine induces oxidative stress and DNA damage to inhibit growth and migration of human lung carcinoma H1299 cells. *J. Agric. Food Chem.* **2011**, *59*, 2284–2290.

(19) Chen, J. Y. F.; Hwang, C. C.; Chen, W. Y.; Lee, J. C.; Fu, T. F.; Fang, K.; Chu, Y. C.; Huang, Y. L.; Lin, J. C.; Tsai, W. H.; Chang, H. W.; Chen, B. H.; Chiu, C. C. Additive effects of C2-ceramide on paclitaxel-induced premature senescence of human lung cancer cells. *Life Sci.* **2010**, *87*, 350–357.

(20) Geback, T.; Schulz, M. M.; Koumoutsakos, P.; Detmar, M. T. Scratch: A novel and simple software tool for automated analysis of monolayer wound healing assays. *BioTechniques* **2009**, *46*, 265–274.

(21) Heney, M.; Alipour, M.; Vergidis, D.; Omri, A.; Mugabe, C.; Thng, J.; Suntres, Z. Effectiveness of liposomal paclitaxel against MCF-7 breast cancer cells. *Can. J. Physiol. Pharmacol.* **2010**, *88*, 1172–1180.

(22) Roussel, E.; Belanger, M. M.; Couet, J. G2/M blockade by paclitaxel induces caveolin-1 expression in A549 lung cancer cells: Caveolin-1 as a marker of cytotoxicity. *Anticancer Drugs* **2004**, *15*, 961–967.

(23) Sharp, D. A.; Lawrence, D. A.; Ashkenazi, A. Selective knock-down of the long variant of cellular FLICE inhibitory protein augments death receptor-mediated caspase-8 activation and apoptosis. *J. Biol. Chem.* **2005**, *280*, 19401.

(24) Takahashi, A. Caspase: Executioner and undertaker of apoptosis. *Int. J. Hematol.* **1999**, *70*, 226–232.

(25) Fan, T. J.; Han, L. H.; Cong, R. S.; Liang, J. Caspase family proteases and apoptosis. *Acta Biochim. Biophys. Sin.* **2005**, *37*, 719–727.

(26) Friedl, P.; Wolf, K. Tumour-cell invasion and migration: Diversity and escape mechanisms. *Nat. Rev. Cancer* **2003**, *3*, 362–374.

(27) Gupta, G. P.; Massagué, J. Cancer metastasis: Building a framework. *Cell* **2006**, *127*, 679–695.